



# A molybdenum(VI) Schiff base complex immobilized on functionalized Fe<sub>3</sub>O<sub>4</sub> nanoparticles as a recoverable nanocatalyst for synthesis of 2-amino-4*H*-benzo[*h*]chromenes

Niaz Monadi<sup>1</sup> · Elham Moradi<sup>1</sup>

Received: 2 October 2017 / Accepted: 28 December 2017  
© Springer International Publishing AG, part of Springer Nature 2018

## Abstract

A dioxomolybdenum(VI) complex of a Schiff base, immobilized on the surface of modified Fe<sub>3</sub>O<sub>4</sub> with a silica coating, has been synthesized and characterized by spectroscopic and microscopic techniques including FTIR, TGA, ICP, SEM, EDX, VSM, and XRD analyses. The catalytic performance of this material has been evaluated for the preparation of 2-amino-4*H*-benzo[*h*]chromenes via the one-pot, three-component reaction of aldehydes, malononitrile, and 1-naphthol under solvent-free conditions. The benefits of this protocol are short reaction time, simple workup procedure, and high yields of products. Also, the synthesized nanocatalyst could be separated easily from the reaction mixture using an external magnet and reused for four consecutive times with only minor degradation of its catalytic performance.

## Introduction

Chromenes (benzopyrones) are an important class of compounds which serve as intermediates in the biological and pharmaceutical chemistry. They are typically prepared by multicomponent reactions (MCRs) [1–4]. MCRs are one of the most important processes for the synthesis of biologically active compounds in modern synthetic chemistry, in which three or more reactants are combined together to generate a desired product. Such compounds are generally prepared by reacting aldehydes, activated methylene compounds, and activated phenols (three-component reaction) in organic solvents [5–8]. Several methods have been reported for the synthesis of these compounds by homogeneous catalysts [9–13], but most of them suffer from drawbacks such as the use of toxic catalysts and bases, difficult recovery and recycling of the catalyst, and lack of general applicability. Therefore, for the synthesis of biological compounds such as chromenes, the development of economical,

eco-friendly, and efficient procedures is an important challenge. An effective strategy to overcome these problems is the use of supported nanocatalysts. Nanoscale materials can provide excellent catalytic activities because of their large surface area. Nanocatalysis can be made of various materials such as metallic nanoparticles, metal oxides, polymers, and carbon-based materials [14–17]. These materials can have special properties including high surface area, excellent catalytic activity, and high absorption capacity, which make them suitable as nanocatalysis [18, 19]. A convenient method for the preparation of nanocatalysis is the heterogenization of homogeneous catalysts by immobilization onto an insoluble nanosupport such as iron oxide nanoparticles (Fe<sub>3</sub>O<sub>4</sub>). Fe<sub>3</sub>O<sub>4</sub> nanoparticles have attracted much attention due to their useful properties including large surface area, superparamagnetism, low toxicity, biocompatibility, and their potential applications in various fields [20–24]. Moreover, this nanosupport can be easily separated from reaction media by the use of an external magnet, giving more effective separation than conventional methods such as filtration or centrifugation.

Schiff base ligands and their complexes are versatile compounds synthesized from the condensation of amines with carbonyl compounds, and widely used for industrial purposes, biological activities, and catalysis of various reactions [25–28]. Despite their high catalytic activity and selectivity, these homogeneous complexes have some problems such as difficult separation of the catalyst, deactivation during the

**Electronic supplementary material** The online version of this article (<https://doi.org/10.1007/s11243-018-0204-x>) contains supplementary material, which is available to authorized users.

✉ Niaz Monadi  
Nimonadi@umz.ac.ir

<sup>1</sup> Department of Inorganic Chemistry, Faculty of Chemistry, University of Mazandaran, Babolsar 47416-95447, Iran

reaction, and difficult separation of the product. Immobilization of the homogeneous catalyst onto a solid support such as  $\text{Fe}_3\text{O}_4$  nanoparticles can overcome these drawbacks [29–32]. With these considerations in mind, we here report the synthesis of 2-amino-4*H*-benzo[*h*]chromenes catalyzed by a dioxomolybdenum(VI) complex supported on  $\text{Fe}_3\text{O}_4$  nanoparticles modified with a silica coating, as a magnetically recoverable nanocatalyst.

## Experimental section

### Materials and physical measurements

All reagents and solvents were purchased from Aldrich, Merck, or Fluka and used without further purification.  $\text{MoO}_2(\text{acac})_2$  was synthesized according to a literature procedure [33]. FTIR spectra were recorded using KBr pellets on a Bruker Vector 22 spectrometer in the range of 400–4000  $\text{cm}^{-1}$ . Thermogravimetric (TGA) analysis was performed on a Perkin Elmer analyzer under nitrogen atmosphere at a heating rate of 10  $^\circ\text{C}/\text{min}$  over a temperature range of 25–800  $^\circ\text{C}$ . Ultrasonic irradiation was carried out with a SONICA-2200 Ep instrument, input 50–60 Hz/305W. The nanoparticles were analyzed using a Holland Philips X Pert X-ray diffraction diffractometer with Cu K $\alpha$  radiation ( $\lambda = 1.5404 \text{ \AA}$ ) in the  $2\theta$  range of  $10^\circ$ – $70^\circ$  at room temperature. Scanning electron microscopy (SEM) images were recorded with a VEGA/TESCAN KYKY-EM3200 microscope. The metal content of the catalysts was measured by inductively coupled plasma atomic emission analysis (ICP-AES, Varian company VISTA-PRO model). Magnetic properties of samples were measured using a vibrating sample magnetometer (VSM, Model MDKB, Meghnatis Danesh Pajoh Kashan Company, Iran).

### Synthesis of $\text{Fe}_3\text{O}_4$ nanoparticles

$\text{Fe}_3\text{O}_4$  nanoparticles were prepared according to the reported method [20, 34]. In a typical procedure,  $\text{FeCl}_3 \cdot 6\text{H}_2\text{O}$  (5.83 g) and  $\text{FeCl}_2 \cdot 4\text{H}_2\text{O}$  (2.147 g) were dissolved in deionized water (150 mL) under an  $\text{N}_2$  atmosphere. Aqueous ammonia (15 mL, 25% w/w) was added dropwise under  $\text{N}_2$ , and the mixture was refluxed for 1 h. After completion of the reaction, the black precipitate was gathered with an external magnet, washed with deionized water ( $3 \times 10 \text{ mL}$ ), and dried in vacuum.

### Synthesis of silica-coated $\text{Fe}_3\text{O}_4$

$\text{Fe}_3\text{O}_4 @ \text{SiO}_2$  nanoparticles were prepared according to the reported method, using the Stöber process [35]. Typically,  $\text{Fe}_3\text{O}_4$  nanoparticles (1 g) were dispersed in a mixture of

deionized water (20 mL) and ethanol (30 mL) under sonication (1 h). Next, tetraethyl orthosilicate (TEOS, 2 mL) and  $\text{NH}_4\text{OH}$  (2.4 mL, 25% w/w) were added dropwise and the mixture was stirred for 3 h at room temperature. The black suspension was decanted using an external magnet and washed several times with deionized water/ethanol. The product  $\text{SiO}_2 @ \text{Fe}_3\text{O}_4$  was dried at 60  $^\circ\text{C}$  for 4 h.

### Functionalization of $\text{Fe}_3\text{O}_4 @ \text{SiO}_2$ with amine

In a typical procedure,  $\text{Fe}_3\text{O}_4 @ \text{SiO}_2$  (0.5 g) was dispersed in ethanol (20 mL) by ultrasonic irradiation and then 1.5 mL 3-aminopropyltriethoxysilane (APTES) was added dropwise. The reaction mixture was refluxed for 12 h under  $\text{N}_2$  atmosphere. The final product designated as  $\text{Fe}_3\text{O}_4 @ \text{SiO}_2\text{-NH}_2$  was decanted using an external magnet and dried at 80  $^\circ\text{C}$  for 4 h [36].

### Synthesis of the nanocatalyst

For preparation of the supported dioxomolybdenum(VI) complex, a mixture of  $\text{Fe}_3\text{O}_4 @ \text{SiO}_2\text{-NH}_2$  (0.3 g),  $\text{MoO}_2(\text{acac})_2$  (1 mmol, 0.33 g), and ethanol (30 mL) was refluxed under  $\text{N}_2$  for 12 h. After completion of the reaction, the green solid was separated with an external magnet and washed three times with deionized water/ethanol. Subsequently, Soxhlet extraction was carried out with ethanol to remove excess/nonreacted metal salt and the final product was dried at 80  $^\circ\text{C}$  for 10 h. The dried pale green solid was denoted as  $\text{Fe}_3\text{O}_4 @ \text{SiO}_2 @ \text{MoO}_2(\text{VI})$  nanocatalyst.

### General procedure for the synthesis of 2-amino-4*H*-benzo[*h*]chromenes

The catalytic activity of  $\text{Fe}_3\text{O}_4 @ \text{SiO}_2 @ \text{MoO}_2(\text{VI})$  for the synthesis of various chromene derivatives was investigated using the following procedure. A mixture of the required aldehyde (1 mmol), 1-naphthol (1 mmol), malononitrile (1 mmol), and nanocatalyst (0.1 g) was heated to 90  $^\circ\text{C}$  under solvent-free conditions. The progress of the reaction was monitored using TLC until the aldehyde spot had disappeared. The mixture was then cooled to room temperature. 5 mL of ethanol was added to the reaction mixture, and it was stirred for 5 min. The nanocatalyst was decanted with the help of an external magnet, washed with ethanol ( $3 \times 15 \text{ mL}$ ), dried, and then reused in the next reaction. The obtained products were filtered off and washed with ethanol three times. The synthesized 2-amino-4*H*-benzo[*h*]chromene derivatives were recrystallized from hot ethanol.

All products were characterized by FTIR and melting point, which were in agreement with the literature [37, 38]. Also,  $^1\text{H}$  and  $^{13}\text{C}$  NMR spectra of some

2-amino-4*H*-benzo[*h*]chromene derivatives are reported (see supporting information).

### Selected spectroscopic data

**2-Amino-4-(4-chlorophenyl)-4*H*-benzo[*h*]chromene-3-carbonitrile (Table 2, entry 3)**  $\nu_{\text{max}}$  (KBr) 3468, 3327, 2192, 1669, 1599, 1407, 1374, 1101  $\text{cm}^{-1}$ ,  $\delta_{\text{H}}$  (400 MHz,  $\text{CDCl}_3$ ): 4.82 (br s, 2H,  $\text{NH}_2$ ), 4.88 (s, 1H, CH), 7.01–8.20 (10H, Ar).

**2-Amino-4-(3-nitrophenyl)-4*H*-benzo[*h*]chromene-3-carbonitrile (Table 2, entry 5)**  $\nu_{\text{max}}$  (KBr) 3470, 3328, 2192, 1666, 1601, 1525, 1406, 1375, 1102  $\text{cm}^{-1}$ ,  $\delta_{\text{H}}$  (400 MHz,  $\text{CD}_3\text{CN}$ ): 5.73 (br s, 2H,  $\text{NH}_2$ ), 5.09 (s, 1H, CH), 7.04–8.30 (10H, Ar).

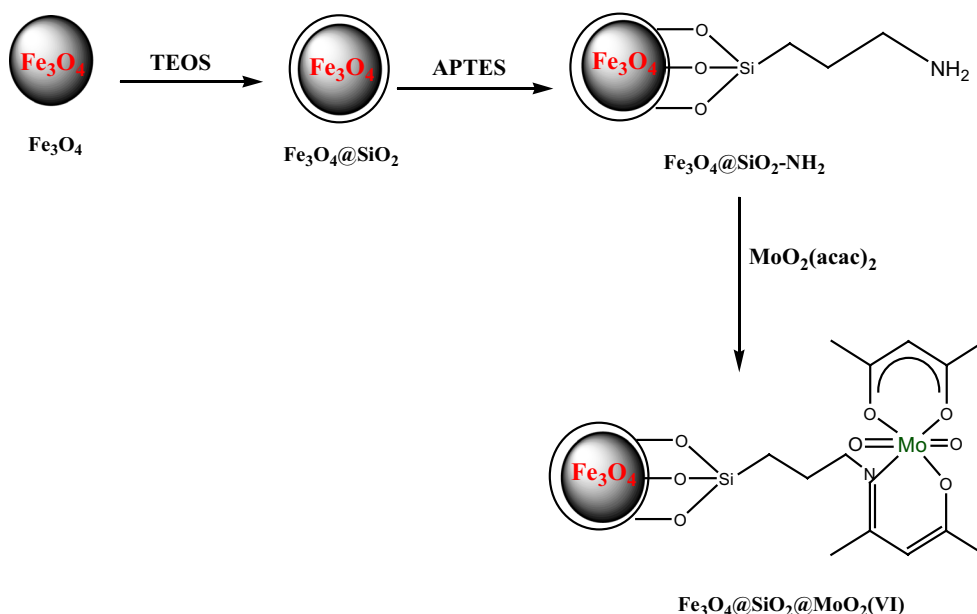
## Results and discussion

### Preparation and characterization of the nanocatalyst

The route for the preparation of the nanocatalyst is shown in Scheme 1. Initially, functionalized magnetic nanoparticles were prepared from Fe(III) and Fe(II) salts via a co-precipitation method, subsequently encapsulated with a silica shell, and functionalized with APTES. Finally, the  $\text{Fe}_3\text{O}_4@ \text{SiO}_2@ \text{MoO}_2(\text{VI})$  nanocatalyst was formed by reaction of the precursors with dioxomolybdenum(VI) acetylacetonate. Both the precursors and final nanocatalyst were characterized by FTIR, TGA, SEM, XRD, EDX, ICP, and VSM.

In the FTIR spectrum of  $\text{Fe}_3\text{O}_4$  (Fig. 1a), an intense broad peak at 578  $\text{cm}^{-1}$  is attributed to the Fe–O stretching mode, while another broad band around 3390  $\text{cm}^{-1}$  is assigned to O–H stretching of the hydroxyl group attached to Fe. The spectrum of  $\text{Fe}_3\text{O}_4@ \text{SiO}_2$  (Fig. 1b) shows the Fe–O stretching vibrations at 577  $\text{cm}^{-1}$  and also two bands at 799 and 1089  $\text{cm}^{-1}$  corresponding to the symmetric and asymmetric stretching vibrations of Si–O–Si groups, respectively. In the spectrum of  $\text{Fe}_3\text{O}_4@ \text{SiO}_2\text{--NH}_2$ , a peak at 2924  $\text{cm}^{-1}$  is ascribed to the  $-\text{CH}_2$  group of APTES; this peak is absent from the spectrum of  $\text{Fe}_3\text{O}_4@ \text{SiO}_2$  (Fig. 1c). The FTIR spectrum of the  $\text{Fe}_3\text{O}_4@ \text{SiO}_2@ \text{MoO}_2(\text{VI})$  nanocatalyst exhibits absorption peaks at 584 and 1091  $\text{cm}^{-1}$ , corresponding to Fe–O and Si–O–Si vibrations, respectively. Furthermore, a new peak at 1635  $\text{cm}^{-1}$  is assigned to the C=N group, While another new peak at 944  $\text{cm}^{-1}$  (stretching vibration of  $\text{O}=\text{Mo}=\text{O}$ ) is evidence of successful grafting of the metal complex onto the surface of the  $\text{Fe}_3\text{O}_4@ \text{SiO}_2\text{--NH}_2$  nanoparticles (Fig. 1d) [35].

In order to confirm immobilization of the molybdenum complex onto the surface of the magnetic support, TGA analysis was also carried out. The TGA curves of  $\text{Fe}_3\text{O}_4$  and  $\text{Fe}_3\text{O}_4@ \text{SiO}_2@ \text{MoO}_2(\text{VI})$  are depicted in Fig. 2. The  $\text{Fe}_3\text{O}_4$  nanoparticles show a weight loss near 100  $^\circ\text{C}$ , of about 3%. This might be due to evaporation of physically adsorbed water. However, there is no further significant weight loss in the range of 100–800  $^\circ\text{C}$  (Fig. 2a). On the other hand, in the TGA curve of  $\text{Fe}_3\text{O}_4@ \text{SiO}_2@ \text{MoO}_2(\text{VI})$  (Fig. 2b), significant weight loss was observed in the range of 250–500  $^\circ\text{C}$  (10.28%), due to the thermal decomposition of the organic groups and metal complex, consistent



**Scheme 1** General route for the preparation of magnetically recoverable nanocatalyst

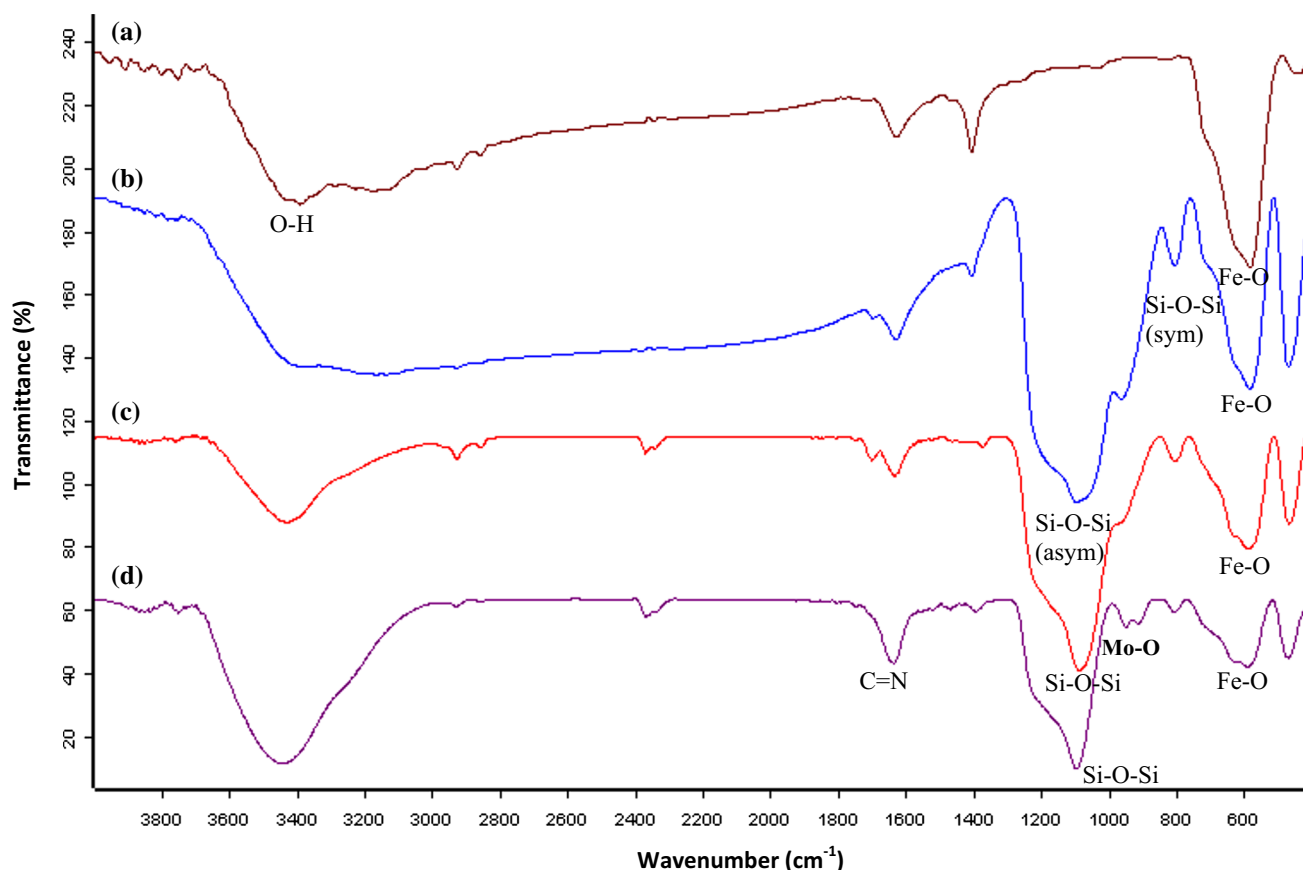


**Fig. 1** FT-IR spectra for  $\text{Fe}_3\text{O}_4$  (a),  $\text{Fe}_3\text{O}_4@\text{SiO}_{32}$  (b),  $\text{Fe}_3\text{O}_4@\text{SiO}_2\text{-NH}_2$  (c), and  $\text{Fe}_3\text{O}_4@\text{SiO}_2@\text{MoO}_2(\text{VI})$  (d)

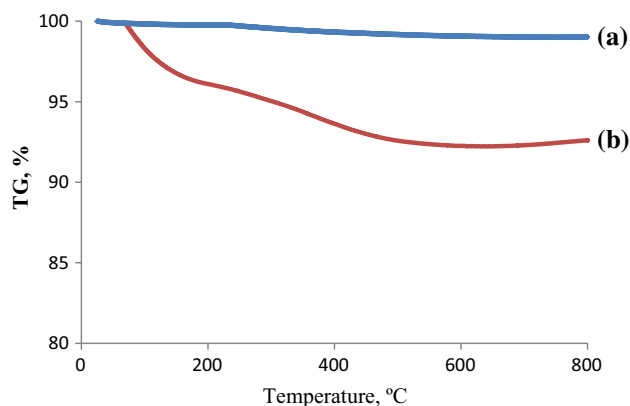


**Fig. 2** TGA diagram for  $\text{Fe}_3\text{O}_4$  (a) and  $\text{Fe}_3\text{O}_4@\text{SiO}_2@\text{MoO}_2(\text{VI})$  (b)

with successful grafting of the metal complex onto the support. Furthermore, based on the weight loss in the TGA curve of  $\text{Fe}_3\text{O}_4@\text{SiO}_2@\text{MoO}_2(\text{VI})$ , the loading of  $\text{MoO}_2(\text{VI})$  complex on the surface was estimated to be  $0.29 \text{ mmol g}^{-1}$ . This is in good agreement with inductively coupled plasma atomic emission spectroscopy (ICP-AES)

measurements, which indicated a molybdenum loading on the magnetic nanocatalyst of  $0.34 \text{ mmol g}^{-1}$ .

In order to obtain information about the magnetic properties of the prepared materials, their magnetization curves were determined by VSM under  $\text{N}_2$  atmosphere at room temperature (Fig. 3). The magnetization curves exhibit no remanence effects, which clearly indicates their superparamagnetic behavior. The magnetization saturation values for  $\text{Fe}_3\text{O}_4$ ,  $\text{Fe}_3\text{O}_4@\text{SiO}_2$ , and  $\text{Fe}_3\text{O}_4@\text{SiO}_2@\text{MoO}_2(\text{VI})$  are 55, 35, and  $25 \text{ emu g}^{-1}$ , respectively. The observed decrease in the magnetization values is consistent with immobilization of the metal complex on the surface of  $\text{Fe}_3\text{O}_4@\text{SiO}_2$  [35]. Also, by using an external magnetic field, the nanocatalyst can be separated from the reaction mixture; when the magnetic field is removed, it is able to redisperse rapidly, indicating that the nanocatalyst possesses good redispersibility and responsiveness.

The XRD patterns of  $\text{Fe}_3\text{O}_4$  and  $\text{Fe}_3\text{O}_4@\text{SiO}_2@\text{MoO}_2(\text{VI})$  are depicted in Fig. 4. The XRD pattern of  $\text{Fe}_3\text{O}_4$  (Fig. 4a) shows six characteristic peaks at  $2\theta = 30.2^\circ$  (220),  $35.5^\circ$  (311),  $43.2^\circ$  (400),  $53.6^\circ$  (422),  $57.1^\circ$  (511), and  $62.7^\circ$  (440), in agreement with magnetite standard data (reference JCPDS card number 19-0629), with an inverse

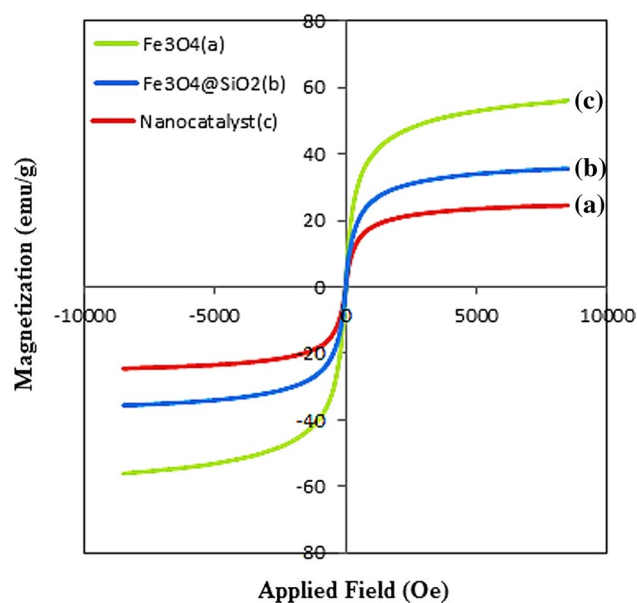


**Fig. 3** Magnetization curves for  $\text{Fe}_3\text{O}_4$  (a),  $\text{Fe}_3\text{O}_4@\text{SiO}_2$  (b), and the  $\text{Fe}_3\text{O}_4@\text{SiO}_2@\text{MoO}_2(\text{VI})$  nanocatalyst (c)

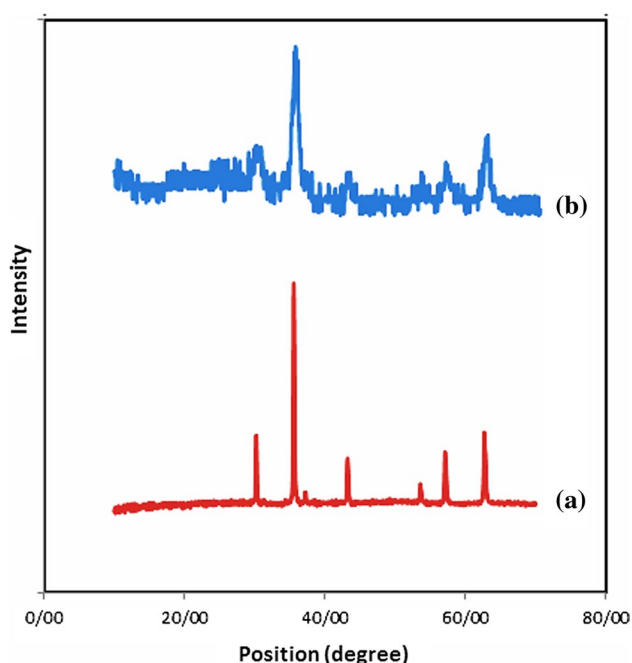


**Fig. 4** XRD pattern for  $\text{Fe}_3\text{O}_4$  (a) and  $\text{Fe}_3\text{O}_4@\text{SiO}_2@\text{MoO}_2(\text{VI})$  (b)

cubic spinel structured without impurity phases. The XRD pattern of the  $\text{Fe}_3\text{O}_4@\text{SiO}_2@\text{MoO}_2(\text{VI})$  nanocatalyst also shows six peaks related to  $\text{Fe}_3\text{O}_4$  (Fig. 4b). Therefore, the magnetic support does not change phase during immobilization of the metal complex. The peak intensities in the XRD pattern of the nanocatalyst are slightly decreased compared

to  $\text{Fe}_3\text{O}_4$ , which is probably due to the shielding effects of silica and the metal complex on the surface [36].

The morphology and size of the prepared materials were evaluated by SEM (Fig. 5). As shown in Fig. 5a, the  $\text{Fe}_3\text{O}_4$  nanoparticles have approximately spherical morphology with some aggregation and vary from 30 to 40 nm in size distribution. The morphology of the nanocatalyst was evaluated by FE-SEM (Fig. 5b), revealing the formation of uniform and mono-dispersed nanoparticles in the range of 90–100 nm. It is obvious that the complexation process has not significantly changed the structure or morphology of the primary support.

The presence of C, N, O, Si, Fe, and Mo in the structure of the  $\text{Fe}_3\text{O}_4@\text{SiO}_2@\text{MoO}_2(\text{VI})$  nanocatalyst was confirmed by EDX analysis (Fig. 6). The element atom ratios of C, N, O, Si, Fe, and Mo are 8.55, 2.84, 62.75, 12.03, 9.58, and 4.27 wt%, respectively. This observation provides further evidence for successful attachment of the dioxomolybdenum complex to the magnetic support.

### Catalytic performance

After synthesis and characterization of the  $\text{Fe}_3\text{O}_4@\text{SiO}_2@\text{MoO}_2(\text{VI})$  nanocatalyst, we have investigated its catalytic activity for the synthesis of 2-amino-4*H*-benzo[*h*]chromenes via the one-pot, three-component reaction of different aldehydes, malononitrile, and 1-naphthol. Initially, we selected the reaction of 2-chlorobenzaldehyde with malononitrile and 1-naphthol as a model for optimization of the conditions (Scheme 2).

The effects of various parameters on catalytic activity such as solvents, amount of the catalyst, and temperature were examined, and the results are collected in Table 1. A control experiment without any catalyst showed negligible conversion even after 24 h (Table 1, entry 1). Hence, the nanocatalyst is essential for this synthesis. Similarly, the use of  $\text{Fe}_3\text{O}_4$ ,  $\text{Fe}_3\text{O}_4@\text{SiO}_2$ ,  $\text{Fe}_3\text{O}_4@\text{SiO}_2-\text{NH}_2$ , and  $\text{MoO}_2(\text{acac})_2$  in place of the  $\text{Fe}_3\text{O}_4@\text{SiO}_2@\text{Mo}(\text{VI})$  nanocatalyst gave no reaction even after 24 h (Table 1, entries 2–5).

The effects of various solvents such as  $\text{H}_2\text{O}$ , ethanol, and methanol were then investigated (Table 1, entries 6–8). Moreover, solvent-free condition was also tested; significant yield and shorter reaction time were observed when this condition was employed (Table 1, entry 10).

To examine the effect of the quantity of nanocatalyst on the catalytic activity, different quantities of  $\text{Fe}_3\text{O}_4@\text{SiO}_2@\text{Mo}(\text{VI})$  were employed (Table 1, entries 9–12). It was found that 0.1 g of nanocatalyst gave maximum yield (96%) under solvent-free conditions at 90 °C (Table 1, entry 10). Lower amounts gave poorer yields, but higher amounts of the nanocatalyst gave no further improvement.



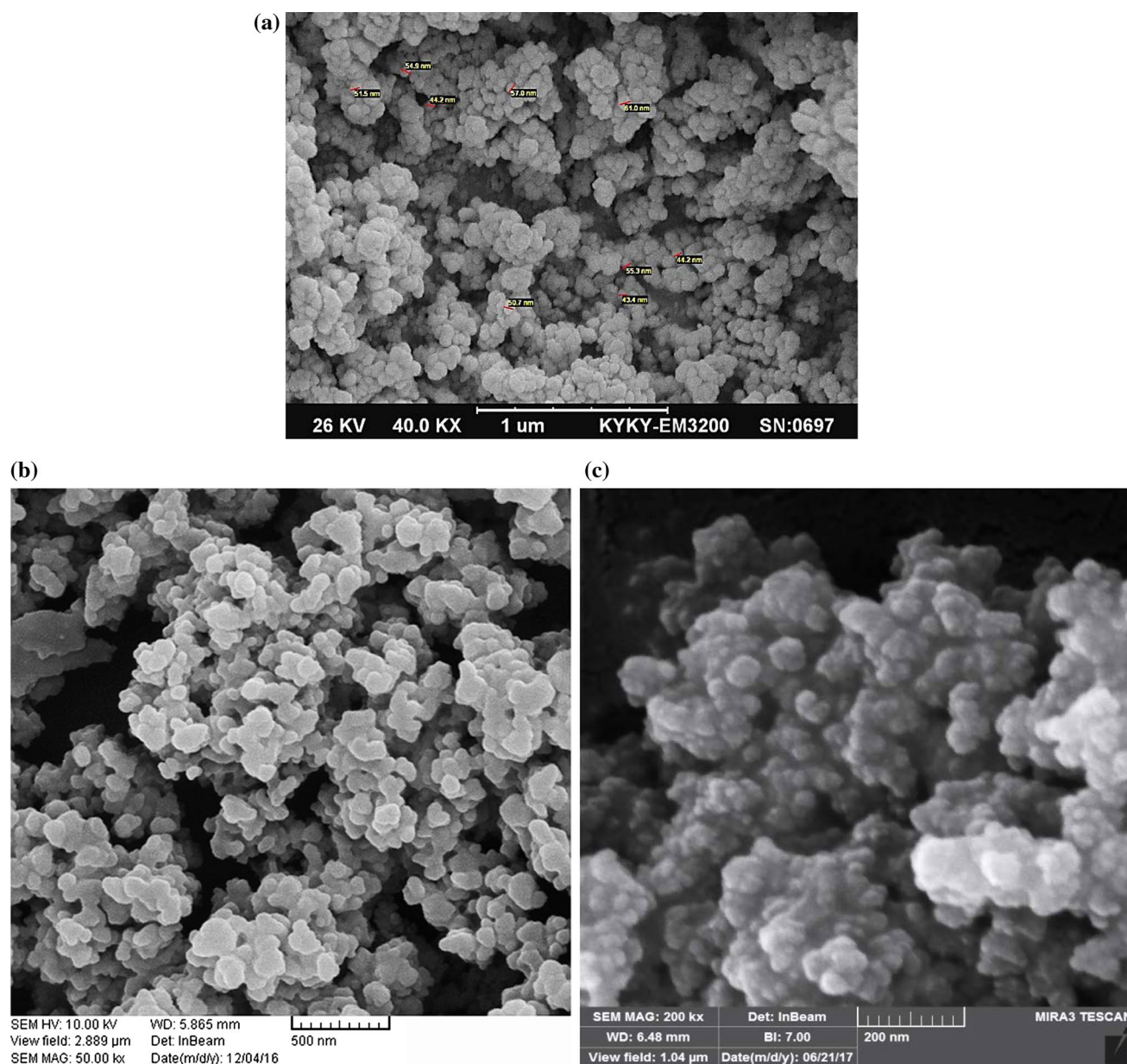


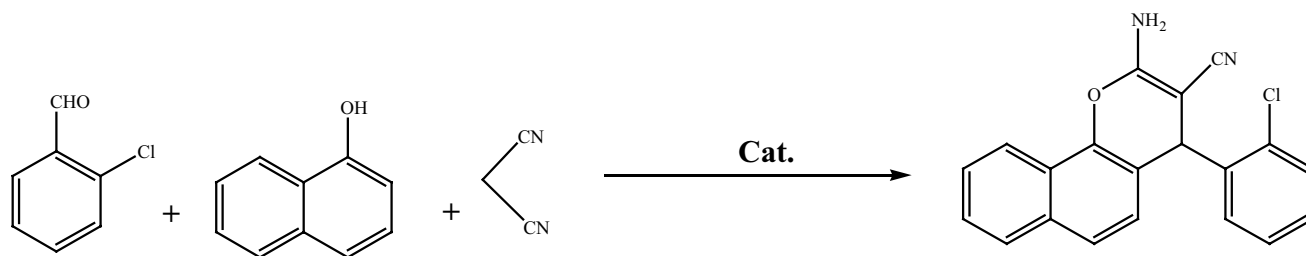
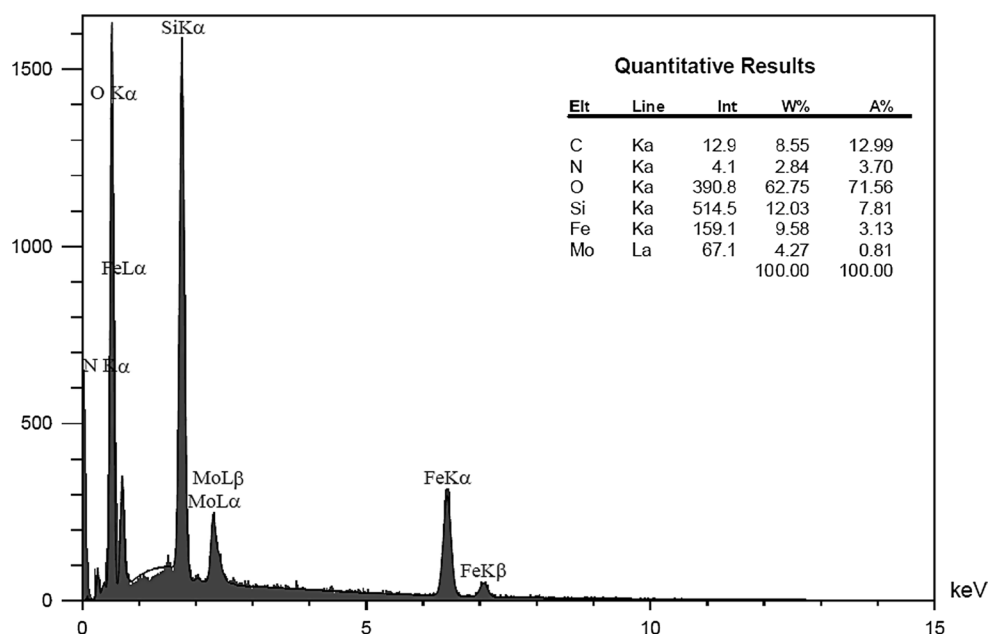
**Fig. 5** SEM image of Fe<sub>3</sub>O<sub>4</sub> (a), Fe<sub>3</sub>O<sub>4</sub>@SiO<sub>2</sub>@MoO<sub>2</sub>(VI) (b), and reused nanocatalyst after 4th run (c)

We next investigated the effect of temperature on the activity of the nanocatalyst; these experiments suggested 90 °C as the optimum temperature. Upon raising the temperature to 125 °C, the yield was decreased (Table 1, Entry 15). Conversely, on running the reaction at room temperature, the yield was decreased to trace (Table 1, entries 13–14). The optimum conditions were thus 0.1 g of the nanocatalyst, under solvent-free conditions at 90 °C.

In order to investigate the versatility of this method, different aromatic aldehydes were treated with malononitrile and 1-naphthol for the synthesis of corresponding 2-amino-4*H*-benzo[*h*]chromenes under the optimized conditions.

The results are summarized in Table 2. Both electron-rich and electron-poor aldehydes reacted well in this method to obtain the corresponding products in good to excellent yields, although the best results were obtained with the electron-withdrawing substituents.

In order to evaluate the present system in more depth, a comparison was made between the current procedure and several published methods for the reaction of 2-chlorobenzaldehyde, malononitrile, and 1-naphthol, as shown in Table 3 [39–44]. The results show that the present method has some merits compared to the previous literature reports in terms of yield, reaction time and temperature. Furthermore, the

**Fig. 6** EDX analysis of the  $\text{Fe}_3\text{O}_4@\text{SiO}_2@\text{MoO}_2(\text{VI})$  nanocatalyst**Scheme 2** One-pot reaction of 2-chlorobenzaldehyde, 1-naphthol, and malononitrile in the presence of nanocatalyst as model reaction**Table 1** Optimization and screening of the nanocatalyst for synthesis of desired product

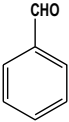
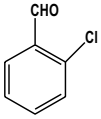
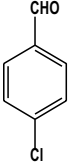
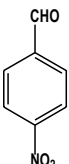
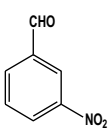
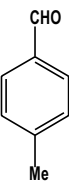
Entry	Catalyst (amount)	Solvent	Temperature (°C)	Time	Yield <sup>a</sup>
1	Without catalyst	No	90	24 h	Trace
2	$\text{Fe}_3\text{O}_4$	No	90	24 h	Trace
3	$\text{Fe}_3\text{O}_4@\text{SiO}_2$	No	90	24 h	Trace
4	$\text{Fe}_3\text{O}_4@\text{SiO}_2\text{-NH}_2$	No	90	24 h	Trace
5	$\text{MoO}_2(\text{acac})_2$	No	90	24 h	Trace
6	$\text{Fe}_3\text{O}_4@\text{SiO}_2@\text{MoO}_2(\text{VI})$ (0.1 g)	$\text{H}_2\text{O}$	90	1:15 h	75%
7	$\text{Fe}_3\text{O}_4@\text{SiO}_2@\text{MoO}_2(\text{VI})$ (0.1 g)	EtOH	90	2 h	50%
8	$\text{Fe}_3\text{O}_4@\text{SiO}_2@\text{MoO}_2(\text{VI})$ (0.1 g)	$\text{CH}_3\text{OH}$	90	2:30 h	40%
9	$\text{Fe}_3\text{O}_4@\text{SiO}_2@\text{MoO}_2(\text{VI})$ (0.05 g)	Solvent-free	90	1:20 h	60%
10	<b><math>\text{Fe}_3\text{O}_4@\text{SiO}_2@\text{MoO}_2(\text{VI})</math> (0.1 g)</b>	<b>Solvent-free</b>	<b>90</b>	<b>1 h</b>	<b>96%</b>
11	$\text{Fe}_3\text{O}_4@\text{SiO}_2@\text{MoO}_2(\text{VI})$ (0.2 g)	Solvent-free	90	50 min	96%
12	$\text{Fe}_3\text{O}_4@\text{SiO}_2@\text{MoO}_2(\text{VI})$ (0.3 g)	Solvent-free	90	45 min	97%
13	$\text{Fe}_3\text{O}_4@\text{SiO}_2@\text{MoO}_2(\text{VI})$ (0.1 g)	Solvent-free	25	24 h	Trace
14	$\text{Fe}_3\text{O}_4@\text{SiO}_2@\text{MoO}_2(\text{VI})$ (0.1 g)	Solvent-free	50	1:30 h	65%
15	$\text{Fe}_3\text{O}_4@\text{SiO}_2@\text{MoO}_2(\text{VI})$ (0.1 g)	Solvent-free	125	2 h	50%

Bold indicates the optimized conditions

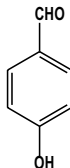
All reactions were carried out with 2-chlorobenzaldehyde (1 mmol), malononitrile (1 mmol), and 1-naphthol (1 mmol)

<sup>a</sup>Isolated yield

**Table 2** Synthesis of 2-amino-4*H*-benzo[*h*]chromenes in the presence of nanocatalyst

Entry	Aldehyde	Time	Yield (%) <sup>a</sup>	Melting point (our work) (°C)	Melting point (literature) (°C)
1.		75 min	87	217–218	217–219 [37, 38]
2.		1 h	96	162–164	162–162 [37, 38]
3.		1 h	92	232–234	232–233 [37, 38]
4.		45 min	94	238–240	238–240 [37, 38]
5.		40 min	92	210–212	212–213 [37, 38]
6.		1:10 h	85	203–205	204–206 [37, 38]

**Table 2** (continued)

Entry	Aldehyde	Time	Yield (%) <sup>a</sup>	Melting point (our work) (°C)	Melting point (literature) (°C)
7.		1 h	90	247–249	246–248 [37, 38]

All reactions were carried out with aldehyde (1 mmol), malonitrile (1 mmol), and 1-naphthol (1 mmol) in the presence of Fe<sub>3</sub>O<sub>4</sub>@SiO<sub>2</sub>@MoO<sub>2</sub>(VI) (0.1 g) under solvent-free condition at 90 °C

<sup>a</sup>Isolated yield

present catalytic system offers other advantages such as mild reaction conditions, stability, easy recovery of the catalyst, and low toxicity compared to other systems.

### Proposed reaction pathway

A plausible reaction mechanism for the synthesis of 2-amino-4*H*-benzo[*h*]chromenes using the nanocatalyst is shown in Scheme 3 [10, 45]. In this mechanism, the nanocatalyst reacts with the aldehyde and the cyano group and activates it for nucleophilic attack. First, malonitrile reacts with the aldehyde to give an  $\alpha$ ,  $\beta$ -unsaturated nitrile (I), which then reacts with 1-naphthol to give the dicyano compound (II). The phenolic OH group then undergoes rapid nucleophilic addition to the C=N moiety, and finally, tautomerization of intermediate (III) gives the 2-aminochromene (IV).

### Reuse of the nanocatalyst

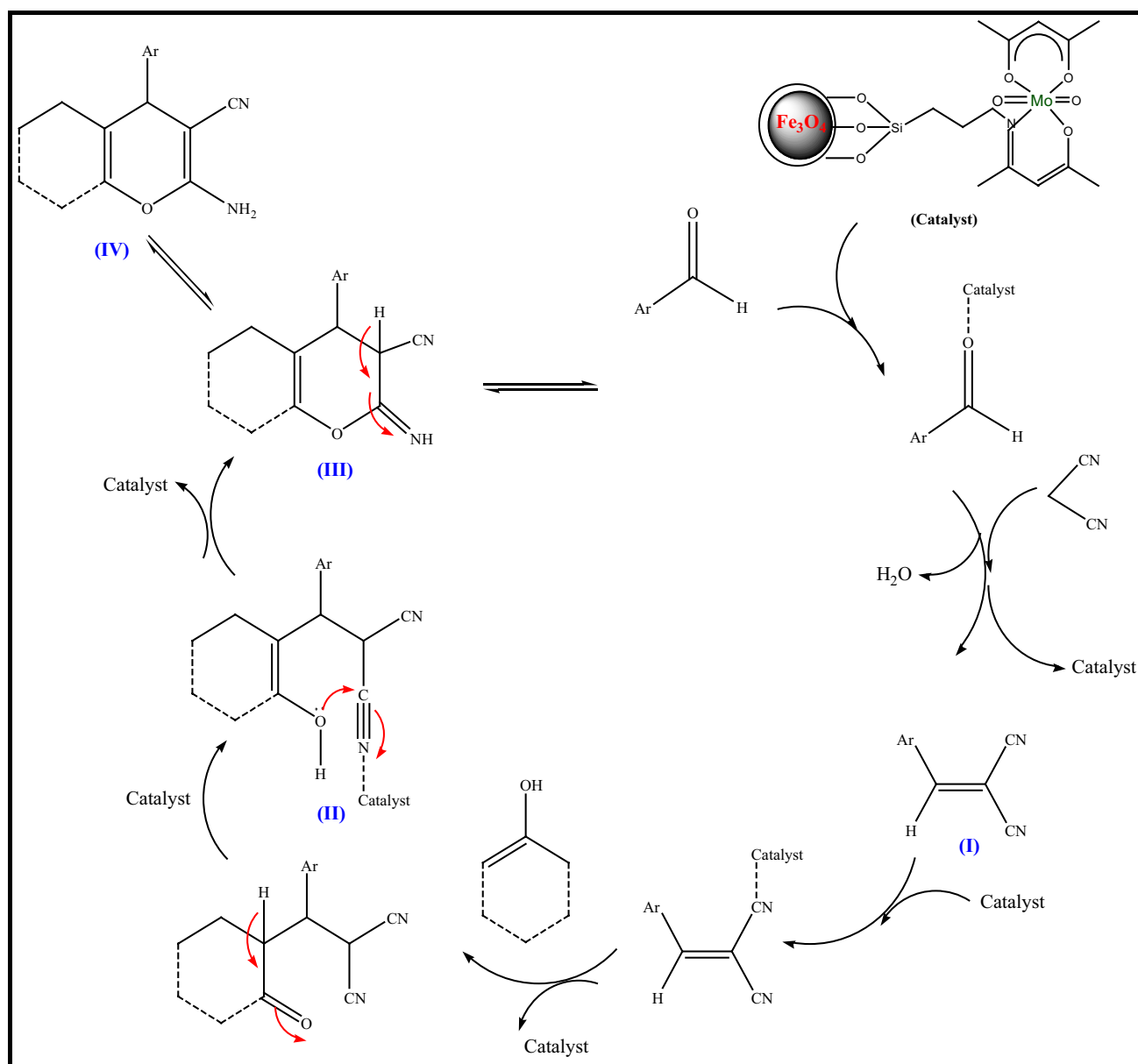
The possibility of recycling the nanocatalyst was examined for the preparation of 2-amino-4*H*-benzo[*h*]chromenes under the optimized conditions (Table 4). The reaction mixture was recovered each time by an external magnet, then washed with hot ethanol (3 × 10 mL), and dried. The nanocatalyst could be reused for at least four runs with only a slight decrease in its catalytic activity. Also, after the fourth catalytic run, SEM imaging was carried out (Fig. 5c). The morphology and structure of the reused nanocatalyst were scarcely changed, consistent with its stability.

To further probe the stability of the nanocatalyst, we carried out leaching tests. The molybdenum leaching in the first and fourth runs was measured by ICP, giving values of 0.001 (0.33%) and 0.002 mmol g<sup>-1</sup> (0.61%), respectively. Hence, the amount of leaching of the nanocatalyst is negligible, and the complex is strongly bonded to the surface of the support.



**Table 3** Comparison of present work with other reported methods in the reaction of aromatic aldehydes, malononitrile, and 1-naphthol

Entry	Catalyst (amount)	Solvent	Temperature	Time	Yield (%)	Ref.
1	HTMAB (10 mol%)	H <sub>2</sub> O	100 °C	4 h	93	[39]
2	[bmim]OH (0.5 mmol)	H <sub>2</sub> O	100 °C	60 min	91	[40]
3	H <sub>14</sub> [NaP <sub>5</sub> W <sub>30</sub> O <sub>110</sub> ] (0.03 g)	H <sub>2</sub> O	100 °C (reflux)	3 h	91	[41]
4	Silica tungstic acid (STA) (0.1 g)	Solvent-free	120 °C	3 h	90	[42]
5	Rochelle salt (0.3 g)	Ethanol	78 °C (reflux)	4–8 h	90	[43]
6	Fe <sub>3</sub> O <sub>4</sub> @SiO <sub>2</sub> @Mo-Schiff base (0.2 g)	Solvent-free	125 °C	60 min	95	[44]
7	(Fe <sub>3</sub> O <sub>4</sub> @SiO <sub>2</sub> @MoO <sub>2</sub> (VI) (0.1 g)	Solvent-free	90 °C	60 min	96	This study

**Scheme 3** Plausible mechanism for the synthesis of 2-amino-4H-benzo[h]chromenes catalysed by Fe<sub>3</sub>O<sub>4</sub>@SiO<sub>2</sub>@MoO<sub>2</sub>(VI)

**Table 4** Reusability test of the  $\text{Fe}_3\text{O}_4@ \text{SiO}_2@ \text{MoO}_2(\text{VI})$  in the model reaction

Entry	Cycle	Yield (%)
1	First run	96
2	Second run	92
3	Third run	88
4	Fourth run	86

## Conclusions

In this work, a molybdenum Schiff base complex has been anchored on the surface of  $\text{Fe}_3\text{O}_4$  nanoparticles modified with a silica shell. This material was investigated as a magnetically recoverable nanocatalyst for the synthesis of 2-amino-4*H*-benzo[*h*]chromenes. The supported dioxomolybdenum nanocatalyst gave high yields of products under solvent-free conditions at 90 °C. The notable advantages of this work are the use of green, nontoxic materials, good stability of the nanocatalyst, and facile reusability.

**Acknowledgements** The authors acknowledge the University of Mazandaran for financial support of this work.

## References

- Dong Z, Liu X, Feng J, Wang M, Lin L, Feng X (2011) *Eur J Org Chem* 2011:137–142
- Yu Y, Guo H, Li X (2011) *J Heterocycl Chem* 48:1264–1268
- Symeonidis T, Chamilos M, Hadjipavlou-Litina DJ, Kallitsakis M, Litinas KE (2009) *Bioorg Med Chem Lett* 19:1139–1142
- Xu Z-Q, Pupek K, Suling WJ, Enache L, Flavin MT (2006) *Bioorg Med Chem* 14:4610–4626
- Syamala M (2009) *Org Prep Proced Int* 41:1–68
- Lin X, Mao Z, Dai X, Lu P, Wang Y (2011) *Chem Commun* 47:6620–6622
- Isambert N, Duque MDMS, Plaquevent J-C, Genisson Y, Rodriguez J, Constantieux T (2011) *Chem Soc Rev* 40:1347–1357
- Dömling A, Ugi I (2000) *Angew Chem Int Ed* 39:3168–3210
- Patra A, Mahapatra T (2008) *J Chem Res* 2008:405–408
- Ren Y-M, Cai C (2008) *Catal Commun* 9:1017–1020
- Bloxham J, Dell CP, Smith CW (1994) *Heterocycles* 38:399–408
- Xs W, Shi Dq Yu, Hz WG, Sj T (2004) *Synth Commun* 34:509–514
- Moafi L, Ahadi S, Bazgir A (2010) *Tetrahedron Lett* 51:6270–6274
- Fagan R, Han C, Andersen J, Pillai S, Falaras P, Byrne A, Dunlop PS, Choi H, Jiang W, O'Shea K, Dionysiou DD (2013) Chapter green nanotechnology: development of nanomaterials for environmental and energy applications. American Chemical Society, Washington
- Chaturvedi S, Dave PN, Shah NK (2012) *J Saudi Chem Soc* 16:307–325
- Cazaux I, Caze C (1993) *Eur Polym J* 29:1615–1619
- Aghajani M, Safaei E, Karimi B (2017) *Synth Metals* 233:63–73
- Grunes J, Zhu J, Somorjai GA (2003) *Chem Commun* 9:2257–2260
- Bell AT (2003) *Science* 299:1688–1691
- Teja AS, Koh P-Y (2009) *Prog Cryst Growth Charact Mater* 55:22–45
- Deng Y-H, Wang C-C, Hu J-H, Yang W-L, Fu S-K (2005) *Colloids Surf A* 262:87–93
- Zhu Y, Stubbs LP, Ho F, Liu R, Ship CP, Maguire JA, Hosmane NS (2010) *ChemCatChem* 2:365–374
- Wu W, He Q, Jiang C (2008) *Nanoscale Res Lett* 3:397
- Alwi R, Telenkov S, Mandelis A, Leshuk T, Gu F, Oladepo S, Michaelian K (2012) *Biomed Opt Express* 3:2500–2509
- Cozzi PG (2004) *Chem Soc Rev* 33:410–421
- Gupta K, Sutar AK (2008) *Coord Chem Rev* 252(12):1420–1450
- Wilkinson SM, Sheedy TM, New EJ (2016) *J Chem Educ* 93:351–354
- Ejidi IP, Ajibade PA (2015) *Rev Inorg Chem* 35:191–224
- Alinezhad H, Tajbakhsh M, Ghobadi N (2015) *Res Chem Intermed* 41:9979–9992
- Gawande MB, Branco PS, Varma RS (2013) *Chem Soc Rev* 42:3371–3393
- Bezaatpour A, Khatami S, Amiri M (2016) *RSC Adv* 6:27452–27459
- Aghajani M, Monadi N (2017) *J Iran Chem Soc* 14:963–975
- Chen GJ, McDonald JW, Newton W (1976) *Inorg Chem* 15:2612–2615
- Wei Y, Han B, Hu X, Lin Y, Wang X, Deng X (2012) *Proc Eng* 27:632–637
- Masteri-Farahani M, Tayyebi N (2011) *J Mol Catal A: Chem* 348:83–87
- Wang Z, Shen B, Aihua Z, He N (2005) *Chem Eng J* 113:27–34
- Khurana JM, Nand B, Saluja P (2010) *Tetrahedron* 66:5637
- Kumar D, Reddy VB, Mishra BG, Rana R, Nadagouda MN, Varma RS (2007) *Tetrahedron* 63:3093
- Jin TS, Zhang JS, Liu LB, Wang AQ, Li TS (2006) *Synth Commun* 36:2009–2015
- Gong K, Wang H-L, Fang D, Liu Z-L (2008) *Catal Commun* 9:650–653
- Heravi MM, Bakhtiari K, Zadsirjan V, Bamoharram FF, Heravi OM (2007) *Bioorg Med Chem Lett* 17:4262–4265
- Farahi M, Karami B, Alipour S, Moghadam LT (2014) *Acta Chim Slov* 61:94–99
- El-Maghraby AM (2014) *Org Chem Int* 2014:715091
- Divsalar N, Monadi N, Tajbakhsh M (2016) *J Nanostruct* 6:312–321
- Khoobi M, Ma'mani L, Rezazadeh F, Zareie Z, Foroumadi A, Ramazani A, Shafiee A (2012) *J Mol Catal A: Chem* 359:74–80